

# Solid State $^{13}\text{C}$ NMR Study of Molecular Complexes of Poly(ethylene oxide) and Hydroxybenzenes

J. Spěváček\*

*Institute of Macromolecular Chemistry, Academy of Sciences of the Czech Republic,  
162 06 Prague 6, Czech Republic*

L. Paternostre, P. Damman, A. C. Draye, and M. Dosière

*Laboratoire de Physico-Chimie des Polymères, Université de Mons-Hainaut, 20, Place du Parc,  
B-7000 Mons, Belgium*

Received October 22, 1997; Revised Manuscript Received March 10, 1998

**ABSTRACT:**  $^{13}\text{C}$  CP/MAS/DD (cross polarization/magic angle spinning/dipolar decoupling) NMR spectra and spin–lattice relaxation times  $T_1$  were measured for highly crystalline stoichiometric complexes of poly(ethylene oxide) (PEO) with resorcinol, 2-methylresorcinol, hydroquinone, and *p*-nitrophenol. It was found that the hydrogen bonding between PEO and hydroxybenzene molecules in molecular complexes results in higher shielding (i.e., lower chemical shifts) of PEO carbons. The largest “upfield” shifts ( $\sim 2.5$  ppm) were observed for PEO/*p*-nitrophenol and PEO/resorcinol complexes where the strongest hydrogen bonds exist, as shown by infrared spectra (OH stretching band). Hydrogen bonding is also the main reason for the lower mobility of PEO chains in molecular complexes with hydroxybenzenes, as detected by  $^{13}\text{C}$   $T_1$  measurements. The very large rigidity of PEO chains in PEO/*p*-nitrophenol complexes is probably due also to other interactions (interaction of other functional groups of *p*-nitrophenol with PEO; pair dipolar interactions between *p*-nitrophenol molecules), in addition to hydrogen bonds.

## Introduction

It is well-known that poly(ethylene oxide) (PEO) forms highly crystalline molecular complexes with various benzene derivatives.<sup>1</sup> Intercalate complexes of PEO with molecules of para-disubstituted benzenes ( $p\text{-C}_6\text{H}_4\text{-XY}$ , where X, Y = F, Cl, Br, I,  $\text{CH}_3$ ), which are only stabilized by weak van der Waals interactions, are one type.<sup>2–4</sup> Another type is crystalline complexes of PEO with hydroxybenzenes such as resorcinol (RES),<sup>5–10</sup> 2-methylresorcinol (2MR),<sup>6,11,12</sup> hydroquinone (HYD),<sup>11,12</sup> and *p*-nitrophenol (PNP),<sup>9,10,13–19</sup> which are capable of forming hydrogen bonds with PEO. In most of the cited papers, phase diagrams, crystal structure, PEO conformation, polymorphism, morphology, and crystallization were studied by a combination of differential scanning calorimetry (DSC), X-ray diffraction, optical microscopy, and infrared (IR) spectroscopy. The results obtained have shown that PEO/RES and PEO/HYD complexes have a 2:1 molar stoichiometry (i.e., 2 PEO monomeric units per 1 RES or HYD molecule),<sup>5,8,12</sup> while the PEO/PNP complex exhibits a 3:2 molar stoichiometry.<sup>13,18</sup> Two complexes ( $\alpha$  and  $\beta$ ) of different composition were found for the PEO/2MR system; the molar stoichiometries are 7:2 and 2:1 for PEO/2MR  $\alpha$  and  $\beta$  complexes, respectively.<sup>12</sup> Two polymorphs were found for PEO/RES and PEO/PNP complexes,<sup>8,17</sup> but in both cases the  $\beta$  form is rather unstable and rapidly transforms into the more stable  $\alpha$  form. Crystal structures of the  $\alpha$  form of the PEO/RES complex (orthorhombic unit cell<sup>9</sup> with  $a = 1.050$  nm,  $b = 1.018$  nm, and  $c$  (chain axis) = 0.978 nm) and the PEO/HYD complex (triclinic unit cell<sup>20</sup> with  $a = 2.077$  nm,  $b = 1.698$  nm,  $c = 1.028$  nm,  $\alpha = 92.2^\circ$ ,  $\beta = 97.6^\circ$ , and  $\gamma = 144.0^\circ$ ) are shown for illustration in Figure 1. IR spectra indicate that while in PEO/RES, PEO/HYD, and both PEO/2MR complexes<sup>8,20</sup> the conformation of PEO chains is similar to that in pure PEO, i.e., TTG (sequence of rotations around C–O, O–C and

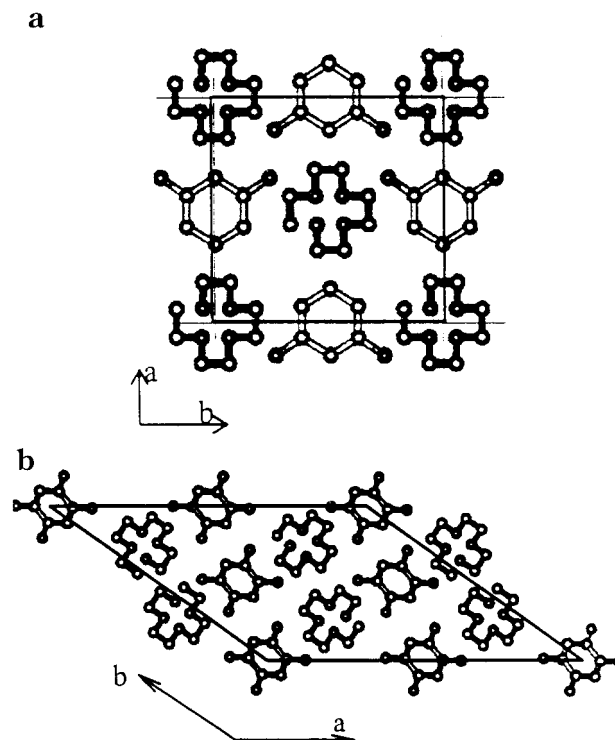


**Figure 1.** Crystal structures of the PEO/RES (a) and PEO/HYD (b) complexes.

C–C bonds, respectively), in the PEO/PNP complex, a somewhat different conformation  $(\text{TTG})_2\text{TTT}$  was proposed on the basis of a normal mode IR analysis and the calculation of the intramolecular energy.<sup>14,18</sup>

Solid state NMR spectroscopy has been applied so far to PEO molecular complexes with benzene derivatives only in several papers.<sup>6,7,11,15,19</sup> Belfiore et al.<sup>6,7,11</sup> studied mainly  $^{13}\text{C}$  signals of hydroxybenzene molecules

as functions of composition in PEO/hydroxybenzene blends, correlating the results with phase diagrams as obtained by DSC. Contrary to Belfiore et al., in the present paper we have used solid state  $^{13}\text{C}$  NMR spectroscopy to characterize interactions and dynamics of PEO chains in molecular complexes with RES, 2MR ( $\alpha$  and  $\beta$ ), HYD, and PNP. An attempt to correlate the obtained results with the strength of hydrogen bonds as determined by IR spectra was also made.

## Experimental Part

**Samples.** PEO of molecular weights 4000 and 6000 (Hoechst) was used in this study. RES and HYD (both from Janssen Chimica) and 2MR and PNP (both from Aldrich) were used as received. Molecular complexes of PEO 6000 with PNP, RES, HYD, and 2MR ( $\alpha$  and  $\beta$ ) were prepared by melting and recrystallizing stoichiometric mixtures of PEO and the respective hydroxybenzene. The molar ratio of PEO monomeric units and the respective hydroxybenzene was 2:1 in PEO/RES (55 wt % of RES), PEO/HYD (55 wt % of HYD) and PEO/2MR- $\beta$  (58.5 wt % of 2MR) complexes. In the PEO/PNP (68 wt % of PNP) complex, this molar ratio was 3:2. In the PEO/2MR- $\alpha$  (42 wt % of 2MR) complex, the content of 2MR was equal to 20.5 molar %, i.e., slightly lower than the stoichiometric value 22.2 molar % corresponding to the 7:2 molar ratio of PEO monomeric unit and 2MR. DSC, X-ray diffraction, and density values indicate that both the PEO complexes of interest and neat PEO samples are highly crystalline (degree of crystallinity  $\geq 85\%$ ).

**NMR Measurements.** Solid state  $^{13}\text{C}$  CP/MAS/DD (cross polarization, magic angle spinning, dipolar decoupling) NMR spectra were measured on a Bruker MSL 200 spectrometer at 50.3 MHz. Samples were measured in 7 mm  $\text{Al}_2\text{O}_3$  or  $\text{ZrO}_2$  rotors and typical measurement conditions were as follows: spinning frequency, 3.3–4 kHz; pulse repetition time, 10 s; spectral width, 20 kHz; number of points, 8K; number of scans, 1800–3600. A proton  $90^\circ$  pulse width was 5  $\mu\text{s}$ , corresponding to a radio frequency (rf) field strength in frequency units of 50 kHz. The detection of the signal of the crystalline phase in neat PEO required a very short contact time (80  $\mu\text{s}$ ).<sup>15</sup> In measurements of  $^{13}\text{C}$  spectra of PEO complexes, a contact time of 1 ms was used (the shape and position of the PEO line in the complex measured with contact time 80  $\mu\text{s}$  was the same). Chemical shifts in  $^{13}\text{C}$  CP/MAS/DD spectra were referred to the carbonyl band of glycine (with a signal at 176.0 ppm) by sample replacement.

$^{13}\text{C}$  spin–lattice relaxation times  $T_1$  were measured with CP by the method of Torchia.<sup>21</sup> The measurement conditions in  $T_1$  measurements were as shown above, only the number of scans was 720–1200. The time delay  $\tau$  equal to 20  $\mu\text{s}$  was used to obtain  $I_0$ ; typically, 12 values of  $\tau$  in the range from 0.1 to 70–100 s were used in  $T_1$  measurements. Simfit software was used for two-exponential fits of magnetization decays.

**IR Measurements.** IR spectra of PEO complexes were obtained on a Bruker IFS 113V FT-IR spectrometer. Thirty-two scans were co-added with a resolution of 2  $\text{cm}^{-1}$ .

**DSC Measurements.** Thermograms were measured on a PYRIS DSC from Perkin-Elmer. The scanning rate was 10  $^\circ\text{C}/\text{min}$ . Sealed aluminum pans containing  $\sim 5$  mg of samples were used. Benzoic acid and indium were used to calibrate the temperature. For the PEO–HYD binary system, the phase diagram was constructed by plotting the observed transition temperature versus the composition of the sample. To ensure the homogeneity of PEO–HYD blends, each sample was melted several times.

## Results and Discussion

**PEO Resonances in  $^{13}\text{C}$  NMR Spectra of Molecular Complexes.** It is known that the  $^{13}\text{C}$  NMR line corresponding to the crystalline phase in neat PEO as measured at room temperature is very broad (line width

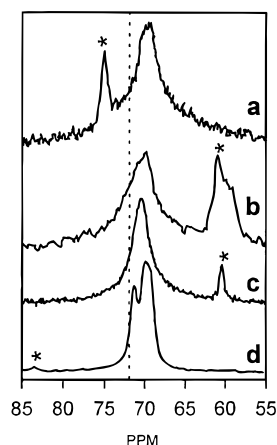


**Figure 2.** PEO resonance in the  $^{13}\text{C}$  CP/MAS/DD NMR spectra of the PEO/RES (a), PEO/HYD (b), PEO/2MR- $\beta$  (c), and PEO/PNP (d) complex measured at 50.3 MHz and 300 K. The dotted line marks the position of the resonance in neat crystalline PEO. Asterisks denote spinning sidebands from hydroxybenzene resonances.

larger than 1 kHz, cf., e.g., Figure 5 in ref 15) and centered at 72 ppm.<sup>15,22,23</sup> The unusual broadness of this line was ascribed to the competition between molecular motion and decoupling,<sup>15,24,25</sup> a mechanism described by Rothwell and Waugh.<sup>26</sup> The shape of the PEO line in  $^{13}\text{C}$  NMR spectra of several PEO/hydroxybenzene complexes at 300 K is shown in Figure 2; the position of the resonance in the crystalline phase of neat PEO is marked by the dotted line. Figure 2a shows the PEO line in the complex PEO/RES. Although this line at  $\sim 69.7$  ppm is much narrower than that for crystalline neat PEO, it is still relatively broad with a line width of 180 Hz. Lines of similar shape were observed also for PEO/HYD (slightly asymmetric line centered at 70.2 ppm) (Figure 2b) and PEO/2MR- $\alpha$  (line centered at 70.5 ppm of somewhat larger width,  $\sim 250$  Hz) complexes. For the PEO/2MR- $\beta$  molecular complex, a narrower line was detected at 70.5 ppm (line width 120 Hz) (Figure 2c). Even narrower are the PEO lines in the PEO/PNP complex, as typical of rigid systems with well-defined structure (Figure 2d). Moreover, two PEO lines at 71.4 and 69.4 ppm were observed for this system; the ratio of integrated intensities of both lines (obtained after deconvolution) is equal to 1:2.

The results mentioned above show that in all PEO complexes with hydroxybenzenes studied, the PEO resonance in  $^{13}\text{C}$  spectra (taking into account the stronger component for PEO/PNP complex) is shifted  $\sim 1.5$ – $2.5$  ppm “upfield” (i.e., toward lower chemical shifts) in comparison to pure crystalline PEO. The magnitude of this shift is larger than chemical shift differences due to the different intermolecular polymer chain packing in the crystal, which usually do not exceed 1 ppm.<sup>27,28</sup> Moreover, only a single stable form was found for the PEO/PNP complex,<sup>17</sup> where two PEO lines were detected in the  $^{13}\text{C}$  NMR spectrum. In principle, this shift could be due to the ring current shielding by interacting hydroxybenzene molecules; a lower chemical shift can be expected for nuclei above the plane of the aromatic ring.<sup>29</sup> This means that the ring current shielding should be the largest if the aromatic ring is parallel to the PEO chain axis, while zero or negative for nuclei in the plane of the aromatic ring. However, the finding that there is no correlation between the observed shift and orientation of hydroxybenzene molecules with respect to the PEO chain axis

and that the largest shift is observed for PEO/PNP and PEO/RES complexes, where the measurements of IR dichroism and X-ray diffraction have shown that the aromatic ring is perpendicular to the chain axis,<sup>8,13,14</sup> exclude this interpretation. The ring current shielding might be responsible for a small "upfield" shift (to 71.2 ppm, cf. ref 15) of the PEO resonance in the PEO/*p*-dichlorobenzene complex, where a 35° angle between the chain axis and aromatic ring was found.<sup>4</sup> A similar orientation was found recently also for the PEO/2MR- $\alpha$  complex<sup>20</sup> and, therefore, approximately half of the observed PEO resonance shift in this system could be due to the ring current shielding. The IR results, showing that the conformation of PEO chains in PEO/RES, PEO/HYD, and both PEO/2MR complexes is very close to TTG<sup>8,20</sup> and that, in the PEO/PNP complex, it is composed of TTG and TTT structures, do not support either the interpretation based on the  $\gamma$ -gauche effect or the assumption of the existence of conformational forms containing one or two gauche C–O bonds.<sup>15,19</sup> Evidently, the observed lower chemical shifts of the PEO carbons in PEO/hydroxybenzene complexes in comparison to the pure PEO or PEO/*p*-dichlorobenzene complex has to be attributed to hydrogen bonds. This is opposite to what is usually reported in the literature<sup>30–33</sup> and what was assumed in an earlier study of the PEO/PNP complex,<sup>19</sup> i.e., that hydrogen bonding leads to higher chemical shifts. On the other hand, higher shielding of PEO in complexes with hydroxybenzenes is in accord with the results of Belfiore et al.,<sup>6,7</sup> who found (and we confirmed by our measurements) that phenolic carbons of RES or 2MR are more shielded in pure compounds where hydrogen bonds are stronger, in comparison to their blends with PEO where hydrogen bonds are weaker. The different stoichiometry of the PEO/RES, PEO/HYD, and PEO/2MR- $\beta$  complexes (molar ratio PEO monomeric unit/hydroxybenzene 2:1) on one hand and the PEO/PNP complex (molar stoichiometry 3:2) on the other explains why one and two NMR signals, respectively, are observed for these systems. In PEO/RES, PEO/HYD, and PEO/2MR- $\beta$ , all oxygen atoms of PEO are involved in hydrogen bonds (PEO oxygen atoms/OH groups ratio 1:1). On the other hand, the observed ratio of integrated intensities 2:1 for two lines in the PEO/PNP complex confirms that the stronger line at 69.4 ppm corresponds to PEO hydrogen-bonded units while the weaker line at 71.4 ppm comes from PEO units which do not form hydrogen bonds; in the latter case, the chemical shift agrees well with what was found earlier for the PEO/*p*-dichlorobenzene complex.<sup>15</sup>

**Spin–Lattice Relaxation Times of PEO Carbons in Molecular Complexes.** For the qualitative investigation of the dynamic structure of PEO/hydroxybenzene complexes we have used the measurements of the spin–lattice relaxation times of PEO carbons. In Figure 3 are shown (as examples) the plots of  $T_1$  decays for the PEO magnetization in three complexes of interest. Similarly to neat PEO, we always observed nonexponential magnetization decays for PEO complexes. They could be fitted well by two exponential components. The fitted  $T_1$  values are given in Table 1; the corresponding intensities of both components are given in Table 1 in parentheses. For the PEO/PNP complex, almost the same magnetization decays (i.e., almost the same  $T_1$  values) were obtained for carbons resonating at 69.4 and 71.4 ppm, proving that both lines correspond to the complexed PEO chains. As usual, the long and short

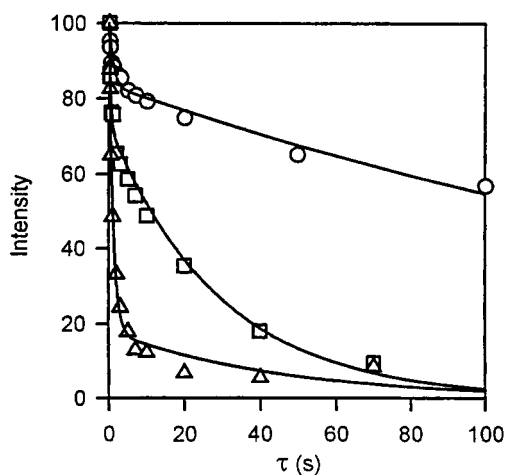


**Figure 3.**  $T_1$  relaxation decays for the magnetization of PEO carbons in the PEO/PNP (○), PEO/2MR- $\beta$  (□), and PEO/HYD (Δ) complex measured at 50.3 MHz and 300 K. Solid lines are two-exponential fits.

**Table 1.**  $^{13}\text{C}$  Spin–Lattice Relaxation Times  $T_1$  of PEO in Molecular Complexes with Hydroxybenzenes

sample	$T_1$ (s) <sup>a</sup>			
	300 K		243 K	
	short comp	long comp	short comp	long comp
PEO <sup>b</sup>	0.3 (24%)	10 (76%)	8 (15%)	176 (85%)
PEO/2MR- $\alpha$	0.25 (40%)	24 (60%)		
PEO/2MR- $\beta$	0.42 (27%)	29.5 (73%)		
PEO/RES	0.5 (30%)	29 (70%)		
PEO/HYD	1.15 (82%)	45 <sup>c</sup> (18%)		
PEO/PNP <sup>d</sup>	1.1 (15%)	236 (85%)	7 (16%)	845 (84%)

<sup>a</sup> Estimated error  $\pm 10\%$ . <sup>b</sup> PEO 4000. <sup>c</sup> Larger experimental error. <sup>d</sup> Stronger component at 69.4 ppm.

$T_1$  components were assigned to the crystalline and amorphous phases, respectively.<sup>34</sup> The  $T_1$  values measured for neat PEO and the PEO/PNP complex at 243 K are longer than those at room temperature, confirming that a longer relaxation time reflects a lower mobility. For most of the studied systems, the intensities of both  $T_1$  components agree reasonably well with the values expected for the crystalline phase (larger intensity) and amorphous phase (smaller intensity). The PEO/HYD complex is an exception; in this system the intensity of the long component is very small (18%) (cf. Figure 3). This results in a rather large experimental error of the respective  $T_1$  value. The origin of the low intensity of the long component in the PEO/HYD complex is not clear. A similar behavior was observed earlier for the PEO/*p*-dichlorobenzene complex at room temperature.<sup>15</sup> A possible explanation could be that the crystalline structure in the PEO/HYD complex is partly destroyed during fast sample spinning used in the MAS technique. For neat PEO, the obtained  $T_1$  values agree well with those reported for its crystalline and amorphous phases in previous studies.<sup>22,35</sup>

From Table 1 it follows that, comparing  $T_1$  values in crystalline phases of the studied systems, the shortest  $T_1$  was found for the crystalline phase of neat PEO, evidently in connection with significant molecular motions with correlation frequencies in the range 10–100 kHz.<sup>15,22–25</sup> The longer and roughly comparable values of  $T_1$  for the crystalline phase in PEO/2MR, PEO/RES, and PEO/HYD complexes (taking into account a large experimental error in the  $T_1$  value of the PEO/HYD complex) indicate a lower PEO mobility in these com-

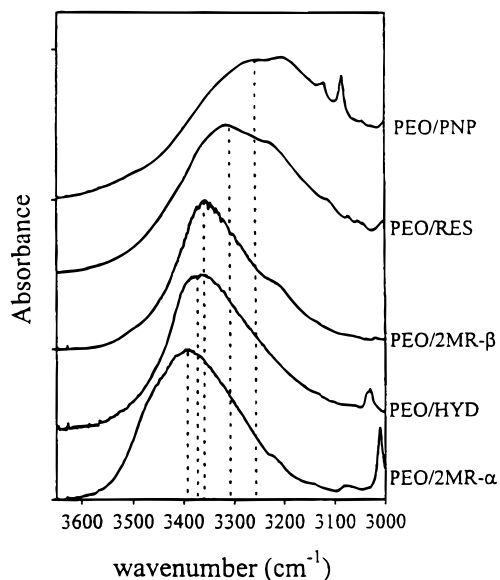


**Figure 4.** IR spectra (OH stretching vibration) of PEO/hydroxybenzene complexes.

**Table 2.**  $^{13}\text{C}$  Chemical Shifts and Spin–Lattice Relaxation Times of PEO Together with Infrared OH Stretching Wavenumbers and Melting Temperatures for Molecular PEO/Hydroxybenzene Complexes

sample	$\delta$ (ppm)	$T_1$ (s) <sup>a</sup>	$\nu_{\text{OH}}$ ( $\text{cm}^{-1}$ )	$T_m^0$ ( $^{\circ}\text{C}$ )
PEO	~72	10 (76%)		69.0
PEO/2MR- $\alpha$	~70.5	24 (60%)	3395	89.2
PEO/2MR- $\beta$	70.5	29.5 (73%)	3360	99.2
PEO/HYD	~70.2	45 <sup>b</sup> (18%)	3365	90.5 <sup>c</sup>
PEO/RES	69.7	29 (70%)	3315	100.2
PEO/PNP	69.4 <sup>d</sup>	236 (85%)	3260	107.9

<sup>a</sup> Long component; its intensity is in parentheses. <sup>b</sup> Larger experimental error because of low intensity. <sup>c</sup> Incongruent melting. <sup>d</sup> Stronger component.

plexes, probably because of hydrogen bonds. The much longer values of  $T_1$  found for the crystalline phase in the PEO/PNP complex show that here the PEO chains are very rigid.

#### Correlation with the Hydrogen Bond Strength.

IR spectroscopy and calorimetry were used for the characterization of hydrogen bond strength in the studied molecular complexes. For similar compounds, it is known that the OH stretching vibration shifts toward lower wavenumbers with increasing strength of hydrogen bonds.<sup>31,36</sup> The IR spectra of PEO/hydroxybenzene complexes between 3000 and 4000  $\text{cm}^{-1}$  are shown in Figure 4. From this figure, it is clear that the hydrogen bond strength increases in the order PEO/2MR- $\alpha$  < PEO/HYD, PEO/2MR- $\beta$  < PEO/RES < PEO/PNP. In contrast to PEO/2MR, PEO/HYD, and PEO/RES complexes, the hydrogen bonds in the PEO/PNP complex are even stronger than those in the neat hydroxybenzene. The equilibrium melting temperatures ( $T_m^0$ ) of the complexes were extrapolated from the  $T_m$  versus  $1/L$  curves<sup>37</sup> ( $T_m$  and  $L$  are the melting temperature and thickness of the crystals) according to the Tammann procedure. As illustrated in Table 2, the melting temperatures reflect the strength of hydrogen bonds. Indeed, a direct correlation between  $T_m^0$  and hydrogen bond strength (as represented by OH stretching wavenumbers) can be found in Table 2. We note, however, that the somewhat lower melting temperature observed for the PEO/HYD complex is due to the incongruent melting. The phase diagram of the PEO–

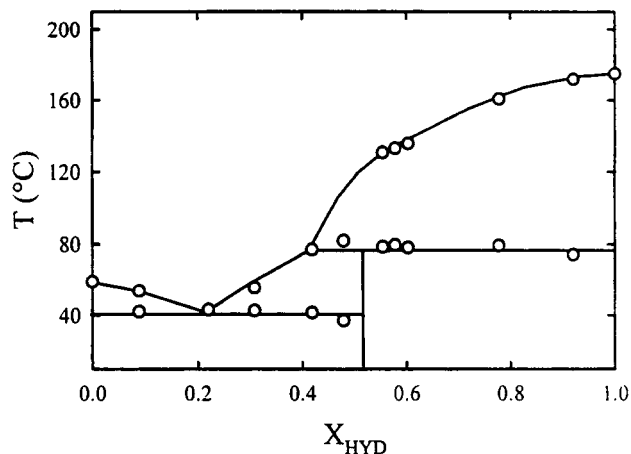


**Figure 5.** Phase diagram of the PEO–HYD binary system;  $X_{\text{HYD}}$  denotes the weight fraction of HYD.

HYD binary system as determined by DSC (Figure 5) shows that at least two crystalline phases (PEO/HYD complex and PEO) coexist at room temperature for all compositions. Moreover, above the peritectic point the crystallization of HYD occurs even for a very fast quench. The existence of the second crystalline phase, which is highly concentrated in PEO (in addition to the PEO/HYD complex), is probably responsible for the asymmetric PEO line shape in the  $^{13}\text{C}$  NMR spectrum of this sample (cf. Figure 2b).

As far as the NMR measurements are concerned, the chemical shifts and spin–lattice relaxation times of PEO carbons for the studied complexes are also summarized in Table 2. Though the precise determination of the PEO chemical shift in some complexes is difficult due to the broadness of  $^{13}\text{C}$  NMR lines, evidently the largest “upfield” shifts were observed for the PEO/RES and PEO/PNP complexes where the hydrogen bonds are strongest. From Table 2, it also follows that excluding neat PEO, the highest mobility (shortest  $T_1$ ) was observed for the PEO/2MR- $\alpha$  complex where the hydrogen bonds are rather weak, while in the PEO/PNP complex with the strongest hydrogen bonds, the mobility of PEO chains is very low. However, an almost 1 order of magnitude difference between  $T_1$  values in the PEO/PNP complex on one hand and in the other PEO/hydroxybenzene complexes on the other hand indicates that the hydrogen bonding probably is not the only mechanism responsible for the low PEO mobility in the PEO/PNP complex. Other functional groups of PNP can also contribute to the interaction with PEO, as indicated by the splitting of the resonances of the protonated carbons of PNP into two components in the PEO/PNP complex in comparison to neat crystalline PNP;<sup>19</sup> such a view is supported by the results of semiempirical quantum-chemical calculations on model systems.<sup>38</sup> Moreover, contrary to other hydroxybenzenes, PNP molecules possess a large dipole moment (5.3 D) and therefore also pair dipolar interactions between PNP molecules (there are two pairs of PNP molecules in the unit cell of a PEO/PNP complex<sup>18</sup>) are probably important, increasing the density of interactions and subsequently hindering the PEO mobility. The large rigidity of PEO chains in the PEO/PNP complex as observed by  $^{13}\text{C}$   $T_1$  measurements can be in direct connection with the existence of stable nonintegral folded PEO chains (NIF) crystals in this system.<sup>1,9,10,16</sup> As shown by calorimetry and time-resolved small-angle X-ray scattering studies, PEO/RES forms NIF crystals, which

rapidly transform into extended-chain crystals or crystals with an integer number of folds (IF). For the PEO/ PNP system, the very low molecular mobility hinders the reorganization of the complex in the solid state. Therefore, NIF crystals of PEO/ PNP are stable in time and never transform into IF crystals.<sup>9,10</sup>

## Conclusions

We have found that the hydrogen bonding between PEO and hydroxybenzene molecules in their stoichiometric complexes results in  $\sim 1.5$ – $2.5$  ppm "upfield" shifts of the PEO line in  $^{13}\text{C}$  NMR spectra. The magnitude of this shift correlates well with the hydrogen bond strength as characterized by IR spectra (OH stretching vibration). The intensity ratio 2:1 observed for two PEO lines at 69.4 and 71.4 ppm in the PEO/ PNP complex, in accord with its 3:2 molar stoichiometry, confirms that the lines correspond to hydrogen-bonded PEO units and those that do not form hydrogen bonds, respectively. Hydrogen bonding is also the main reason for the lower mobility of PEO chains in PEO/hydroxybenzene complexes in comparison to neat crystalline PEO, as detected by  $^{13}\text{C}$  spin–lattice relaxation measurements. However, a very large rigidity of PEO chains found for the PEO/ PNP molecular complex is probably also due to other mechanisms (interaction of other functional groups of PNP with PEO; pair dipolar interactions between PNP molecules), in addition to hydrogen bonds.

**Acknowledgment.** Grant No. A1050602 of the Grant Agency of the Academy of Sciences of the Czech Republic and the grants of the Belgian Funds for Scientific Research, which enabled two one-month stays at the Université de Mons-Hainaut in 1996 and 1997 for J.S., are gratefully acknowledged. The authors also thank Dr. H. Pavlíková for her help in NMR relaxation measurements.

## References and Notes

- (1) Dosièrè, M. *J. Macromol. Sci., Phys. B* **1996**, *35*, 303.
- (2) Point, J. J.; Coutelier, C. *J. Polym. Sci., Polym. Phys. Ed.* **1985**, *22*, 231.
- (3) Point, J. J.; Damman, P. *Makromol. Chem., Macromol. Symp.* **1990**, *39*, 301.
- (4) Point, J. J.; Jasse, B.; Dosièrè, M. *J. Phys. Chem.* **1986**, *90*, 3273.
- (5) Myasnikova, R. M.; Titova, E. F.; Obolonska, E. S. *Polymer* **1980**, *21*, 403.
- (6) Cheng, C.; Belfiore, L. A. *Polym. News* **1990**, *15*, 39.
- (7) Belfiore, L. A.; Lutz, T. J.; Cheng C.; Bronnimann, C. E. *J. Polym. Sci., Part B: Polym. Phys.* **1990**, *28*, 1261.
- (8) Delaite, E.; Point, J. J.; Damman, P.; Dosièrè, M. *Macromolecules* **1992**, *25*, 4768.
- (9) Paternostre, L.; Damman, P.; Dosièrè, M.; Bourgaux, C. *Macromolecules* **1996**, *29*, 2046.
- (10) Paternostre, L.; Damman, P.; Dosièrè, M. *Macromolecules* **1997**, *30*, 3946.
- (11) Belfiore, L. A.; Ueda, E. *Polymer* **1992**, *33*, 3833.
- (12) Paternostre, L.; Damman, P.; Dosièrè, M. *Macromol. Symp.* **1997**, *114*, 205.
- (13) Point, J. J.; Damman, P. *Macromolecules* **1992**, *25*, 1184.
- (14) Damman, P.; Point, J. J. *Macromolecules* **1994**, *27*, 3919.
- (15) Spěváček, J.; Straka, J. *Makromol. Chem., Macromol. Symp.* **1993**, *72*, 201.
- (16) Damman, P.; Point, J. J. *Macromolecules* **1993**, *26*, 1722.
- (17) Damman, P.; Point, J. J. *Macromolecules* **1995**, *28*, 2050.
- (18) Damman, P.; Point, J. J. *Polym. Int.* **1995**, *36*, 117.
- (19) Spěváček, J.; Suchopárek, M. *Macromol. Symp.* **1997**, *114*, 23.
- (20) Paternostre, L. Ph.D. Thesis, Université de Mons-Hainaut, 1997.
- (21) Torchia, D. A. *J. Magn. Reson.* **1978**, *30*, 613.
- (22) Dechter, J. J. *J. Polym. Sci., Polym. Lett. Ed.* **1985**, *23*, 261.
- (23) Schantz, S. *Macromolecules* **1997**, *30*, 1419.
- (24) VanderHart, D. L.; Earl, W. L.; Garroway, A. N. *J. Magn. Reson.* **1981**, *44*, 361.
- (25) Johansson, A.; Tegenfeldt, J. *Macromolecules* **1992**, *25*, 4712.
- (26) Rothwell, W. P.; Waugh, J. S. *J. Chem. Phys.* **1981**, *74*, 2721.
- (27) Axelsson, D. E. In *High-Resolution NMR Spectroscopy of Synthetic Polymers in Bulk*; Komoroski, R. A., Ed.; VCH Publishers: Deerfield Beach, FL, 1986; Chapter 5.
- (28) Voelkel, R. *Angew. Chem., Int. Ed. Engl.* **1988**, *27*, 1468.
- (29) Knowles, P. F.; Marsh, D.; Rattle, H. W. E. *Magnetic Resonance of Biomolecules*; John Wiley & Sons: London, 1976; Chapter 2.
- (30) Kalinowski, H.-O.; Berger, S.; Braun, S. *Carbon-13 NMR Spectroscopy*; John Wiley & Sons: Chichester, U.K., 1988; Chapter 3.
- (31) Vinogradov, S. N.; Linnell, R. H. *Hydrogen Bonding*; Van Nostrand Reinhold Co.: New York, 1971; Chapters 3 and 4.
- (32) Imashiro, F.; Maeda, S.; Takegoshi, K.; Terao, T.; Saika, A. *Chem. Phys. Lett.* **1982**, *92*, 642; **1983**, *99*, 189.
- (33) Terao, T.; Maeda, S.; Saika, A. *Macromolecules* **1983**, *16*, 1535.
- (34) Bovey, F. A.; Mirau, P. A. *NMR of Polymers*; Academic Press: San Diego, 1996; Chapter 5.
- (35) O'Gara, J. F.; Nazri, G.-A.; MacArthur, D. M. *Solid State Ionics* **1991**, *47*, 87.
- (36) Pimentel, G. C.; Sederholm, C. H. *J. Chem. Phys.* **1956**, *24*, 639.
- (37) Paternostre, L.; Damman, P.; Dosièrè, M. To be published.
- (38) Dybal, J.; Spěváček, J. To be published.

MA971552D